Supporting Information

Breaking the Symmetry of Interfacial Molecules with Push-Pull Substituents Enables 19.67% Efficiency Organic Solar Cells Featuring Enhanced Charge Extraction

Lei Liu[a, b, +], Fengyi Yu[a, d, +], Dingqin Hu[a, c, *], Xue Jiang[a, b], Peihao Huang[a, d], Yulu Li[a, d], Gengsui Tian[a, d], Hongliang Lei[a, d], Shiwen Wu[a, b], Kaihuai Tu[a, b], Chen Chen[a, b], Teng Gu[a], Yao Chen[a, d], Tainan Duan[a, d, *], Zeyun Xiao[a, d, *]

[a]Chongqing Institute of Green and Intelligent Technology, Chinese Academy of Sciences, Chongqing 400714, P. R. China.

[b]Chongqing Jiaotong University, Chongqing 400074, P. R. China.

[c]School of Energy and Environment, Department of Materials Science and Engineering, Centre for Functional Photonics (CFP), City University of Hong Kong, Kowloon Tong, Hong Kong, China

[d] University of Chinese Academy of Sciences, Beijing 100049, P. R. China.

[+] These authors contributed equally to this work.

***Corresponding author**

E-mail address: Z. Xiao, xiao.z@cigit.ac.cn; D. Hu, dingqihu@cityu.edu.hk; T. Duan, tnduan@cigit.ac.cn

Content

Experiment section

1. Materials:

The indium-doped tin oxide (ITO)-coated glass (≤15 Ω/square) was purchased from Liaoning Youxuan New Energy Technology Co. Ltd. PM6, BTP-eC9, Y6, L8-BO, and PNDIT-F3N were purchased from Solarmer Energy Inc. PEDOT:PSS was purchased from Xi'an Yuri Solar Energy Technology Co.Ltd. The raw materials 3,6-dibromocarbazole was purchased from Adamas, 3,4-dimethoxyphenylboronic acid was purchased from Leyan, and diethyl 2-bromoethylphosphonate was purchased from BIDD Pharmaceutical Company. All the chemicals were used as received without further purification. All reactions and manipulations were carried out under argon atmosphere with the use of standard Schlenk techniques. All these solvents used here were commercially available from Chongqing Chuandong Chemical.

2. Device fabrication

The OSCs were fabricated with the traditional structure: ITO/ HTLs /activelayer / PNDIT-F3N /Ag. After being cleaned with deionized water, acetone, and isopropanol, the ITO glass was treated with the UV-Ozone for 15 min. For the PEDOT: PSS device: the PEDOT:PSS solution was spin-coated at 6000 rpm onto the ITO substrates for 20 seconds. Then the PEDOT:PSS layer was heated at 150 ℃ for 10 min in air. For the SAMs device: the BrDECz (0.4 mg/mL in ethanol), BrCz (0.4 mg/mL in ethanol), DECz (0.4 mg/mL in THF) solution was applied directly onto the ITO substrate for 15 s followed by a spin-coating step at 3000 rpm for 30 s. The ITO/SAMs substrate was then placed onto a hotplate and annealed at 100 °C for 5 min. PM6:Y6 (ratio 1:1.2, 17 mg/mL in chloroform with 12mg/ml 1,4-diiodobenzene) were spun at 2800 rpm for 30 s to obtain an active-layer, then the active layer was annealed at 90 °C for 2 min. PM6:L8-BO (ratio 1:1.2, 17 mg/mL in chloroform with 12mg/ml 1,4-diiodobenzene) were spun at 3000 rpm for 30 s to obtain an active-layer, then the active layer was annealed at 90 °C for 5 min. PM6:BTP-eC9 (ratio 1:1.2, 16 mg/mL in chloroform and added 11 mg/ml 1,4-diiodobenzene) were spun at 2700 rpm

for 30 s to obtain an active-layer, then the active layer was annealed at 90 °C for 5 min. With the PNDIT-F3N (0.5 mg/mL in methanol added 0.5%acetic acid, 2000 rpm) spin-coated on the active layer, the devices were finally transferred to the evaporation tank to deposit 100 nm Ag. The active area with calibration was 0.1 cm^2.

3. Nuclear magnetic resonance (NMR) spectra.

Spectra were recorded on a Bruker Avance III Ultra shield Plus instrument (600 MHz) for ^1H and (150 MHZ) for ^{13}C spectra. Proton (^1H)NMR information is given in the following format: multiplicity (s, singlet; d, doublet; t, triplet; q, quartet; qui, quintet; sept, septet; m, multiplet), coupling constant(s) (J) in Hertz (Hz), and the number of protons. Carbon (^{13}C) NMR spectra are reported in ppm (δ) relative to residual DMSO (δ 77.16).

4. High-resolution mass spectrometry (HRMS).

Data for SAM molecules were obtained using Japan Shimadzu LCMS-IT-TOF mass spectrometer.

5. UV-visible (UV-vis) absorption.

UV-visible spectra were recorded on a PerkinElmer LAMBDA 365 UV-Vis spectrophotometer.

6. Electrochemical cyclic voltammogram.

Cyclic Voltammetry (CV) was conducted using CIH660e electrochemical workstation with glassy carbon working electrode, platinum wire auxiliary electrode, and Ag/Ag^+ glass electrode used as the reference electrode. Ag/Ag^+ reference electrode was utilized ferrocene/ferrocenium (Fc/Fc^+) redox couple with Fc/Fc^+ set relative to 4.8 eV vacuum level. All CV curves were obtained through casting thin films (from DMSO solution of SMA materials) on a glassy carbon electrode.

7. Contact angle measurement.

Contact angles of two different solvents (water and formamide) were measured on DSA-100 liquid droplet on the pure film (donor/acceptor) using a shape analysis instrument (KRÜSS Scientific). Miscibility of the two components in the mixture could be estimated based on the solubility parameters (δ) of each material, calculated using the formula: $\delta = K\sqrt{\gamma}$ where γ is the surface energy of the material, and K is a proportionality constant (K= 116×10^3 $m^{1/2}$).

8. X-ray photoelectron spectroscopy (XPS).

XPS was performed at Thermo Scientific K-Alpha. Appropriate-sized samples (typically 5 x 5 mm in length and width) were mounted on the sample holder and placed into the Thermo Scientific K-Alpha XPS instrument sample chamber. The sample was transferred to the analysis chamber when the pressure in the sample chamber was less than 2.0×10^{-7} mbar. The spot size was set to 400 μm, the operating voltage to 12 kV, and the filament current to 6 mA. For full-spectrum scans, the pass energy was 150 eV with a step size of 1 eV; for narrow-spectrum scans, the pass energy was 50 eV with a step size of 0.1 eV.

9. Ultraviolet photoelectron spectroscopy (UPS).

The UPS analysis was performed utilizing the Thermo Fisher Scientific ESCALAB XI+ apparatus, situated within an ultra-high vacuum environment where the baseline pressure was maintained at an extremely low level of 1 × 10-10 mbar. The continuous supply of photons for the UPS investigation was sourced from the monochromatized He I α radiation produced by the discharge lamp, delivering photon energies precisely at 21.22 electron volts. The criteria for preparing the samples were consistent with the protocols established for the XPS studies, ensuring comparability between the two spectroscopic techniques.

10. Density functional theory (DFT) computation.

The molecular geometry optimizations and ESP distribution of BrDECz, DECz and BrCz were performed by Gaussian 16 [1] at B3LYP/6-311G** level.

$$E_{ads} = E_{iso/surf} - E_{iso} - E_{surf}$$

The adsorption energies (E_{ads}) were calculated by the following equation:

Here, the three terms on the right are the total energy of surface covered with adsorbates, the total energy of isolated adsorbate molecule, and the total energy of the bare surface. A vacuum spacing of over 15 Å was added to each interfacial bulk model to avoid possible interactions between the periodic slabs. The ITO (001) surface was selected for the construction of interfacial models, with 4 In atoms randomly replaced by Sn atoms. The surface is saturated by H. The formula for the ITO surface model is $In_{44}Sn_4O_{72}H_{24}$.

The DFT calculations for the interfacial models were carried out using Vienna Ab initio Simulation Package (VASP 5.4.4) software[2]. We utilized the Perdew–Burke–Ernzerhof (PBE) exchange-correlation functional[3] and Projector Augmented Wave (PAW) pseudopotentials[3] for structure optimization and total energy calculations. A plane–wave cutoff energy of 500 eV and a 1×2×1 Γ-centered k-mesh were selected. The one-dimensional planar-average charge density difference was calculated by VASPKIT[3]. To take into account van der Waals interaction, the vdW-DF2 functional was used.

11. Materials synthesis:

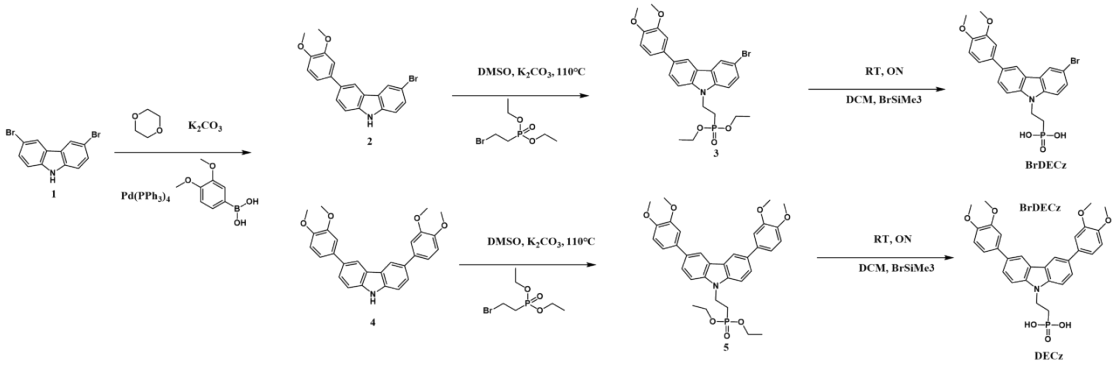

Scheme S1. Synthetic routes of BrDECz and DECz.

11.1 Synthesis of 3-bromo-6-(3,4-dimethoxyphenyl)-9H-carbazole (2)

The compound 1 (2.00 g, 6 mmol), 3,4-dimethoxyphenylboronic acid (2.78 g, 13 mmol), and potassium carbonate (3.30 g, 24 mmol) were dissolved in a mixed solvent of dioxane (50 mL) and water (5 mL) at a ratio of 10:1. A catalytic amount of the $pd(pph_3)_4$ (160 mg, 0.1 mmol) was then added, and the mixture was stirred at 90°C for 24 hours. The reaction mixture was extracted with ethyl acetate (EA) and saturated brine. The organic layer was collected, dried over anhydrous sodium sulfate (Na_2SO_4), filtered, and concentrated under reduced pressure. Purification by silica gel column chromatography using a 1:1 eluent of dichloromethane (DCM) and petroleum ether (PE) yielded a white solid compound 2(600 mg, yield 51%). **^{1}H NMR** (600 MHz, DMSO-d_6) δ 11.45 (s, 1H), 8.52 (s, 1H), 8.48 (s, 1H), 7.75 (d, J = 8.5 Hz, 1H), 7.56 (d, J = 8.4 Hz, 1H), 7.53 (d, J = 10.4 Hz, 1H), 7.49 (d, J = 8.6 Hz, 1H), 7.36 (s, 1H), 7.29 (d, J = 8.3 Hz, 1H), 7.06 (d, J = 8.3 Hz, 1H), 3.92 (s, 3H), 3.82 (s, 3H). **^{13}C NMR** (151 MHz, DMSO-d_6) δ 149.60, 148.37, 139.82, 139.39, 134.42, 131.91, 128.45, 125.74, 125.16, 123.53, 122.60, 119.12, 118.87, 113.50, 112.82, 111.89, 111.10, 111.07, 56.12.

11.2 Synthesis of diethyl(2-(3-bromo-6-(3,4-dimethoxyphenyl)-9H-carbazol-9-yl) ethyl)phosphonate (3)

The white compound 2 (200 mg, 0.52 mmol), diethyl 2-bromoethylphosphonate (141 mg, 0.57 mmol), and potassium carbonate (143 mg, 1.04 mmol) were dissolved in DMSO. The solution was heated and reacted at 110°C overnight. The reaction mixture was then extracted with ethyl acetate (EA) and saturated brine. The organic phase was collected and purified using EA:petroleum ether (PE) at a ratio of 2:1 as the eluent, yielding a pale yellow oil compound 3 (143 mg, 50% yield). **^{1}H NMR** (600 MHz, DMSO-d_6) δ 8.56 (s, 1H), 8.53 (s, 1H), 7.84 (d, J = 6.8 Hz, 1H), 7.65 (d, J = 8.6 Hz, 1H), 7.62 (d, J = 10.5 Hz, 1H), 7.59 (d, J = 8.7 Hz, 1H), 7.38 (s, 1H), 7.32 (d, J = 2.1 Hz, 1H), 4.63 (dt, J = 14.2, 7.2 Hz, 2H), 3.99 (d, J = 1.0 Hz, 4H), 3.92 (s, 3H), 3.83 (s, 3H), 2.37 – 2.29 (m, 2H), 1.11 (t, J = 7.0 Hz, 6H). **^{13}C NMR** (151 MHz,

DMSO) δ 149.63, 148.49, 139.57, 139.25, 134.11, 132.38, 128.56, 125.79, 125.02, 123.59, 122.44, 119.15, 118.96, 112.80, 112.00, 111.64, 111.04, 110.30, 61.66, 60.24, 56.10, 40.40, 40.27, 40.13, 39.99, 39.85, 39.71, 39.57, 18.69, 17.76, 6.87.

11.3 Synthesis of (2-(3-bromo-6-(3,4-dimethoxyphenyl)-9H-carbazol-9-yl)ethyl) phosphonic acid (BrDECz)

The compound 3 was added to anhydrous dichloromethane (DCM). Trimethylsilyl bromide was then added at room temperature, and the mixture was stirred overnight. Upon completion of the reaction, it was quenched by pouring into methanol. The mixture was then concentrated under reduced pressure until only a small amount of liquid remained. Water was added, resulting in the formation of a white precipitate. After standing for 5 minutes, the product BrDECz was isolated by filtration, yielding 140 mg (98% yield). **^{1}H NMR** (600 MHz, DMSO-d_6 δ 8.56 (s, 1H), 8.53 (s, 1H), 7.84 (d, J = 8.6 Hz, 1H), 7.63 (d, J = 6.1 Hz, 2H), 7.56 (d, J = 8.7 Hz, 1H), 7.37 (s, 1H), 7.32 (d, J = 8.3 Hz, 1H), 7.08 (d, J = 8.3 Hz, 1H), 4.60 – 4.56 (m, 2H), 3.92 (s, 3H), 3.83 (s, 3H), 2.10 – 2.03 (m, 2H). **^{13}C NMR** (151 MHz, DMSO-d_6) δ 149.61, 148.47, 139.51, 139.16, 134.13, 132.37, 128.72, 125.95, 124.98, 123.74, 122.41, 119.19, 119.13, 112.83, 111.71, 111.62, 111.09, 110.05, 66.86, 56.13, 38.18, 28.19, 27.32. **HRMS-ESI** m/z Calcd for $C_{22}H_{22}BrNO_5P$ $[M+H]^+$: 490.03, found 490.04.

11.4 Synthesis of3,6-bis(3,4-dimethoxyphenyl)-9H-carbazole (4)

The compound 1 (2.00 g, 6 mmol), 3,4-dimethoxyphenylboronic acid (2.78 g, 13 mmol), and potassium carbonate (3.30 g, 24 mmol) were dissolved in a mixed solvent of dioxane (50 mL) and water (5 mL) at a ratio of 10:1. A catalytic amount of the $Pd(PPh_3)_4$ (160 mg, 0.1 mmol) was added, and the mixture was heated and reacted at 90°C for 24 hours. The reaction mixture was then extracted with ethyl acetate (EA) and saturated brine. The organic layer was separated, dried over anhydrous sodium sulfate (Na_2SO_4), filtered, and concentrated under reduced pressure. The residue was purified by silica gel column chromatography using a 1:1 eluent of dichloromethane (DCM) and petroleum ether (PE), yielding 300 mg of white solid compound 4 (26% yield). **^{1}H NMR** (600 MHz, DMSO-d_6) δ 11.30 (s, 1H), 8.53 (s, 2H), 7.71 (d, J = 6.6

Hz, 2H), 7.55 (d, J = 8.4 Hz, 2H), 7.36 (s, 2H), 7.31 (d, J = 8.3 Hz, 2H), 7.07 (d, J = 8.3 Hz, 2H), 3.92 (s, 6H), 3.83 (s, 6H). **^{13}C NMR** (151 MHz, DMSO-d_6) δ 149.59, 148.31, 139.93, 134.76, 131.59, 125.12, 123.75, 119.21, 118.68, 112.83, 111.73, 111.18, 56.17, 56.13, 40.45, 40.31, 40.17, 40.03, 39.89, 39.76, 39.62.

11.5 Synthesis of (2-(3,6-bis(3,4-dimethoxyphenyl)-9H-carbazol-9-yl)ethyl) phosphonic acid（DECz）

The subsequent synthesis steps were similar to those used in the synthesis of BrDECz, yielding a white product (138 mg, 60% yield). **^{1}H NMR** (600 MHz, DMSO-d_6) δ 8.57 (s, 1H), 7.80 (d, *J* = 8.3 Hz, 1H), 7.62 (d, *J* = 8.5 Hz, 1H), 7.37 (s, 1H), 7.33 (d, *J* = 8.5 Hz, 1H), 7.09 (d, *J* = 8.3 Hz, 1H), 4.61 (q, *J* = 7.9 Hz, 1H), 3.92 (s, 3H), 3.83 (s, 3H), 2.09 (dt, *J* = 17.3, 7.9 Hz, 1H). **^{13}C NMR** (151 MHz, DMSO-d_6) δ 149.60, 148.41, 139.62, 134.48, 132.07, 125.36, 123.64, 119.30, 118.95, 112.84, 111.22, 109.84, 56.20, 56.14, 40.40, 40.27, 40.13, 39.99, 39.85, 39.71, 39.57, 38.10, 28.29, 27.43. **HRMS-ESI** m/z Calcd for $C_{30}H_{31}NO_7P$ $[M+H]^+$: 548.18, found 548.18.

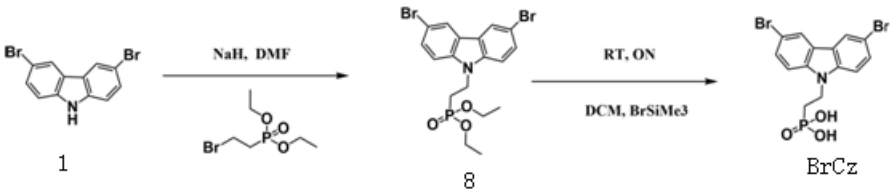

Scheme. S2 Synthetic routes of SAM BrCz.

11.6 Synthesis of (2-(3,6-dibromo-9H-carbazol-9-yl)ethyl)phosphonic acid

The reagent 1 (1.00 g, 3 mmol) was added to 30 mL of DMF. Sodium hydride (NaH, 0.16 g, 3.3 mmol) was slowly added, and the mixture was pre-stirred for 30 minutes. Afterward, diethyl 2-bromoethylphosphonate (0.90 g, 3.6 mmol) was added, and the reaction was stirred at room temperature overnight. Upon completion of the reaction, extraction was performed using ethyl acetate (EA) and saturated brine. The solution was then concentrated under reduced pressure, and the residue was purified by column chromatography using a 1:1 eluent of ethyl acetate (EA) and petroleum ether

(PE), yielding 0.83 g of white solid compound 8 (56% yield). **^{1}H NMR** (600 MHz, DMSO-d_6) δ 8.45 (d, J = 2.0 Hz, 2H), 7.61 (d, J = 6.7 Hz, 2H), 7.56 (d, J = 8.7 Hz, 2H), 4.57 (dt, J = 14.5, 7.1 Hz, 2H), 3.86 (t, J = 7.1 Hz, 4H), 2.34 – 2.25 (m, 2H), 1.05 (t, J = 7.1 Hz, 6H). **^{13}C NMR** (151 MHz, DMSO-d_6) δ 139.11, 129.28, 123.82, 123.64, 112.19, 112.01, 61.68, 61.64, 37.85, 37.45, 37.42, 25.00, 24.09, 16.47, 16.43. Compound 8 was then dissolved in anhydrous dichloromethane. An excess of trimethylsilyl bromide was added dropwise, and the reaction was allowed to proceed overnight. Upon completion of the reaction, methanol was added to quench it. The solution was then concentrated under reduced pressure until a small amount of liquid remained, after which distilled water was added. This resulted in the precipitation of a solid. After standing for 5 minutes, the solid was collected by filtration, yielding white solid product BrCz (0.73 g, 98% yield). **^{1}H NMR** (600 MHz, DMSO-d_6) δ 8.49 (d, J = 2.1 Hz, 1H), 7.65 (ddd, J = 8.7, 3.2, 2.0 Hz, 1H), 7.58 (t, J = 9.1 Hz, 1H), 4.59 – 4.53 (m, 1H), 2.17 – 2.01 (m, 1H). **^{13}C NMR** (151 MHz, DMSO) δ 139.08, 129.45, 124.02, 123.66, 111.99, 111.94, 60.67, 49.11, 40.44, 40.30, 40.16, 40.03, 39.89, 39.75, 39.61. **HRMS-ESI** m/z Calcd for $C_{14}H_{13}Br_2NO_3P$ $[M+H]^+$: 431.89, found 431.89.

12. Supporting Figures

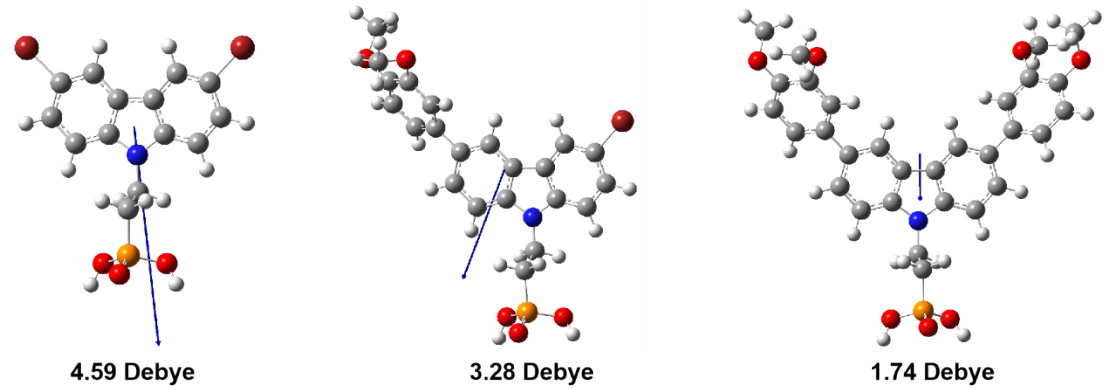

Figure S1. Dipole moments of the SAM molecules.

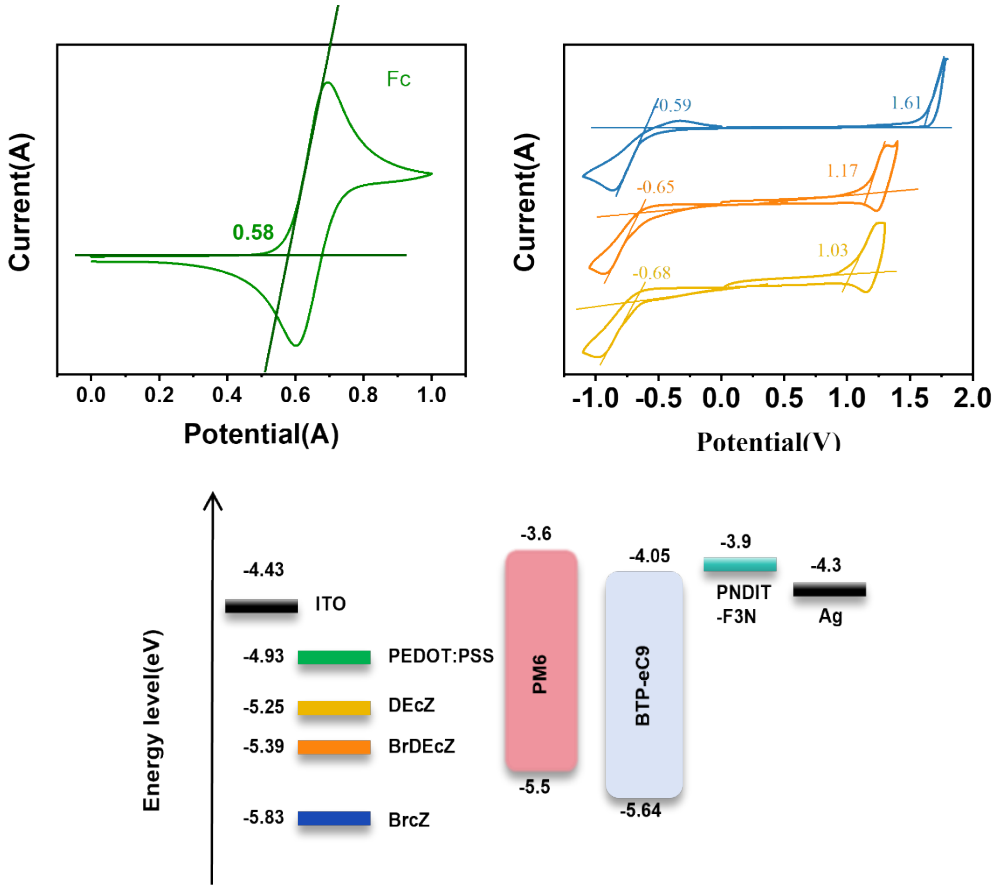

Figure S2. (a) Oxidation and reduction scans of Fc. (b) The CV of SAMs films. The corresponding potential values are extracted by the crossing points of the two tangent lines. (c) HOMO and LUMO energy level diagrams derived from values obtained by cyclic voltammetry.

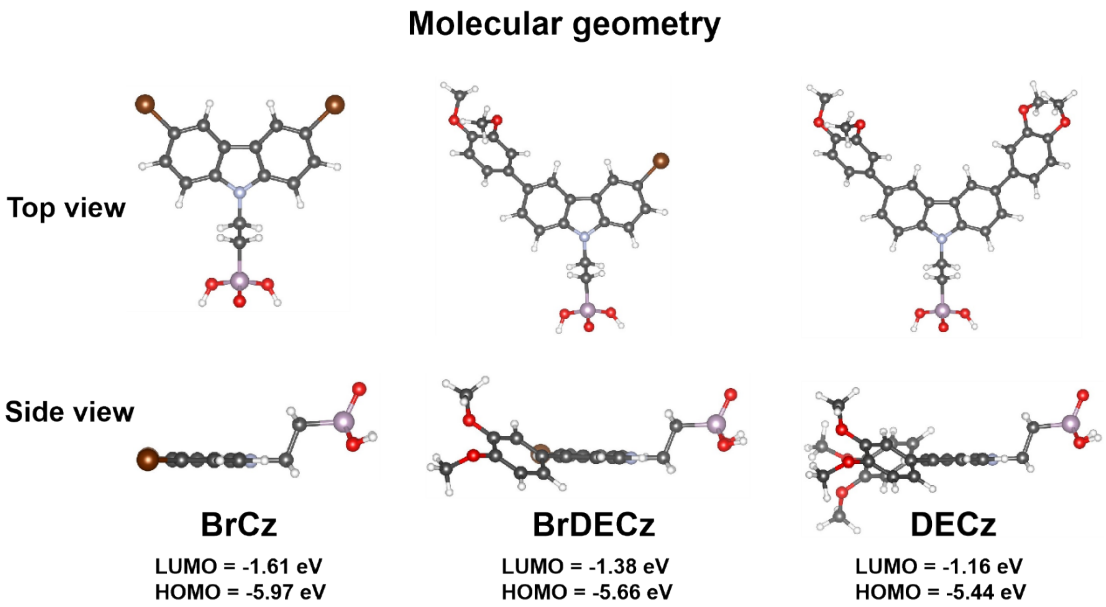

Figure S3. HOMO and LUMO energy levels calculated by DFT.

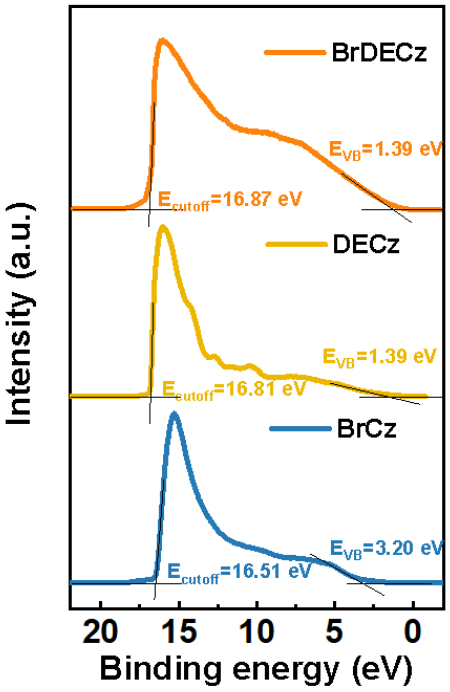

Figure S4. UPS spectra of SAM modified ITO.

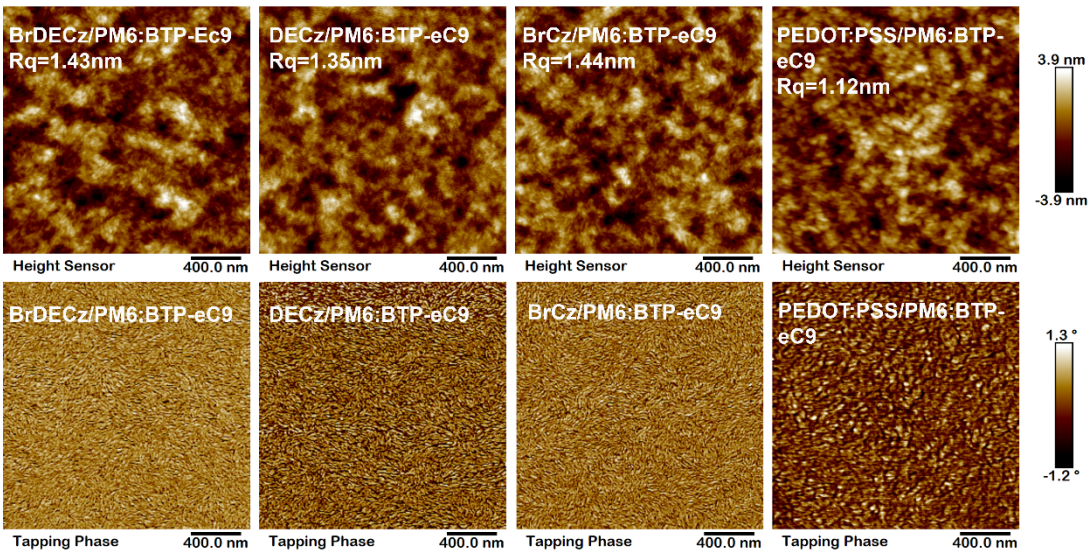

Figure S5. The AFM images of the active layer on SAMs and PEDOT:PSS.

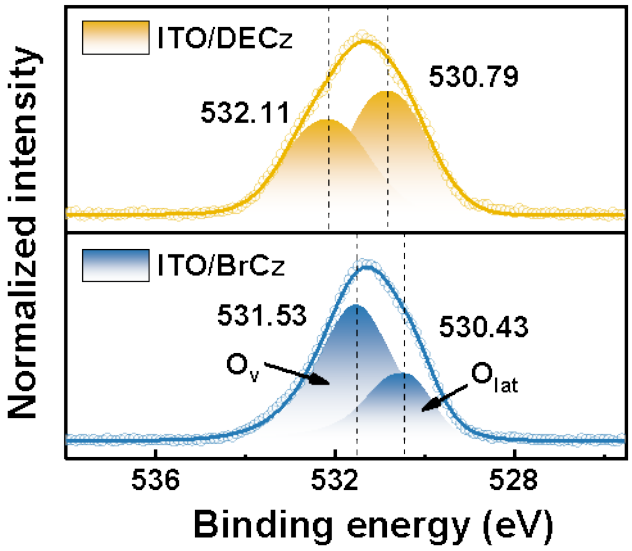

Figure S6. XPS signals of O1s for ITO/BrCz, and ITO/DECz.

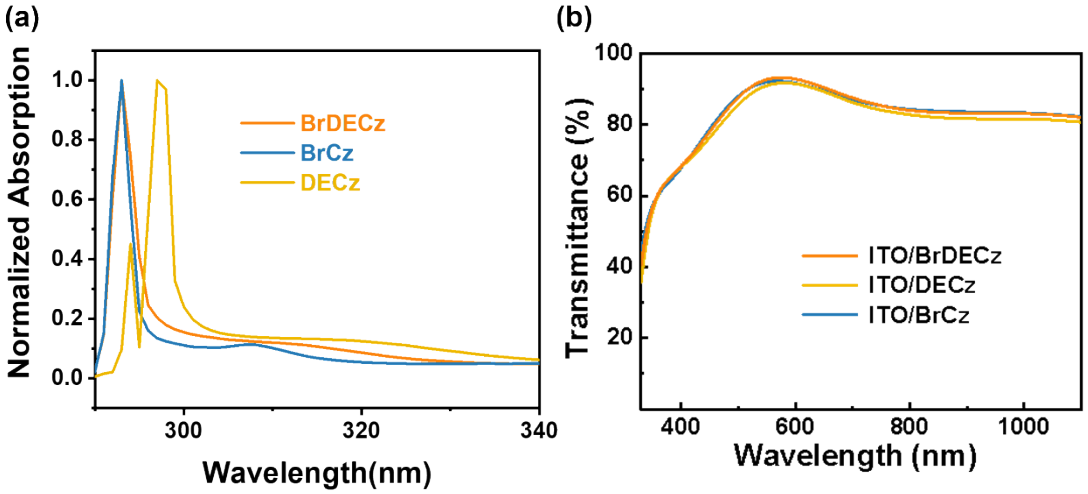

Figure S7. (a) Normalized film absorption spectra of the interfacial materials. (b) The transmittance of the interfacial materials.

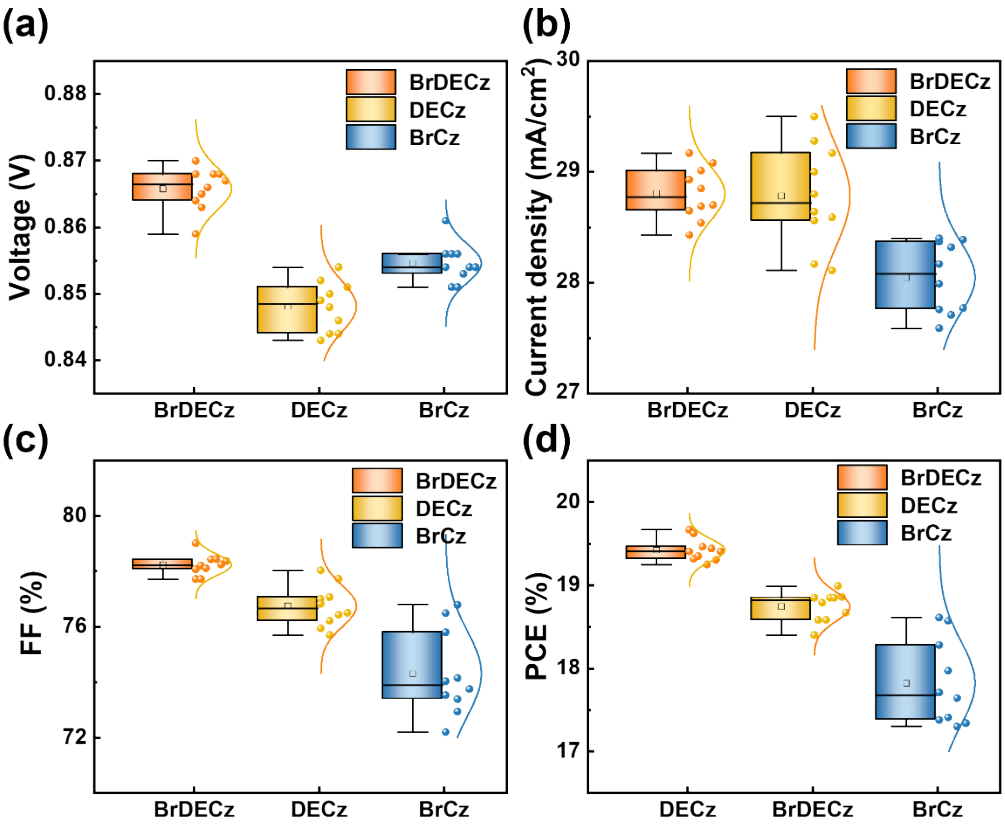

Figure S8. Photovoltaic performance variations for 10 individual devices based on SAMs using PM6:BTP-eC9 as active layer: (a) V_{OC} (b) J_{SC} (c) FF and (d) PCE.

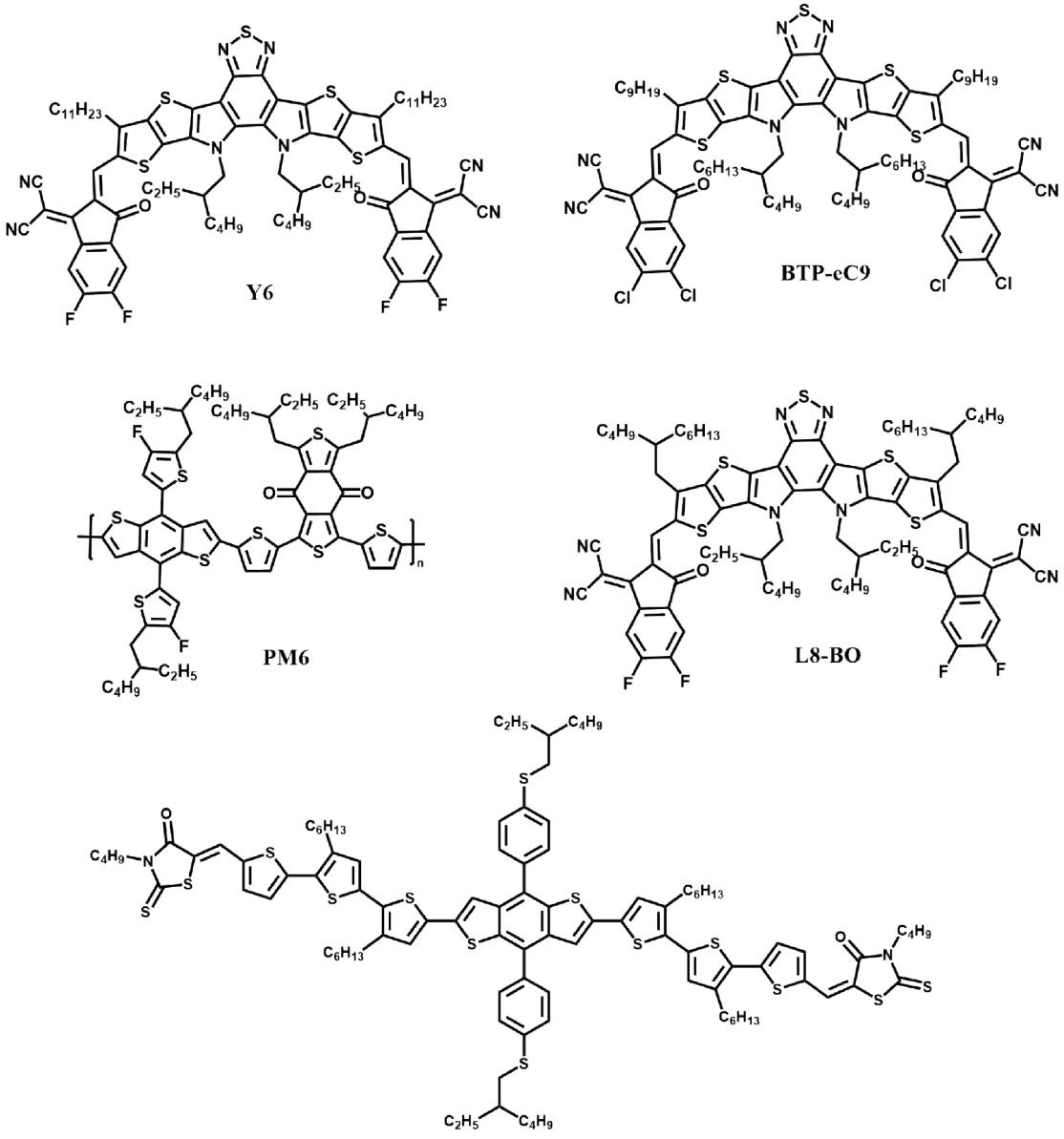

Figure S9. The chemical structures of the materials used in OSC devices.

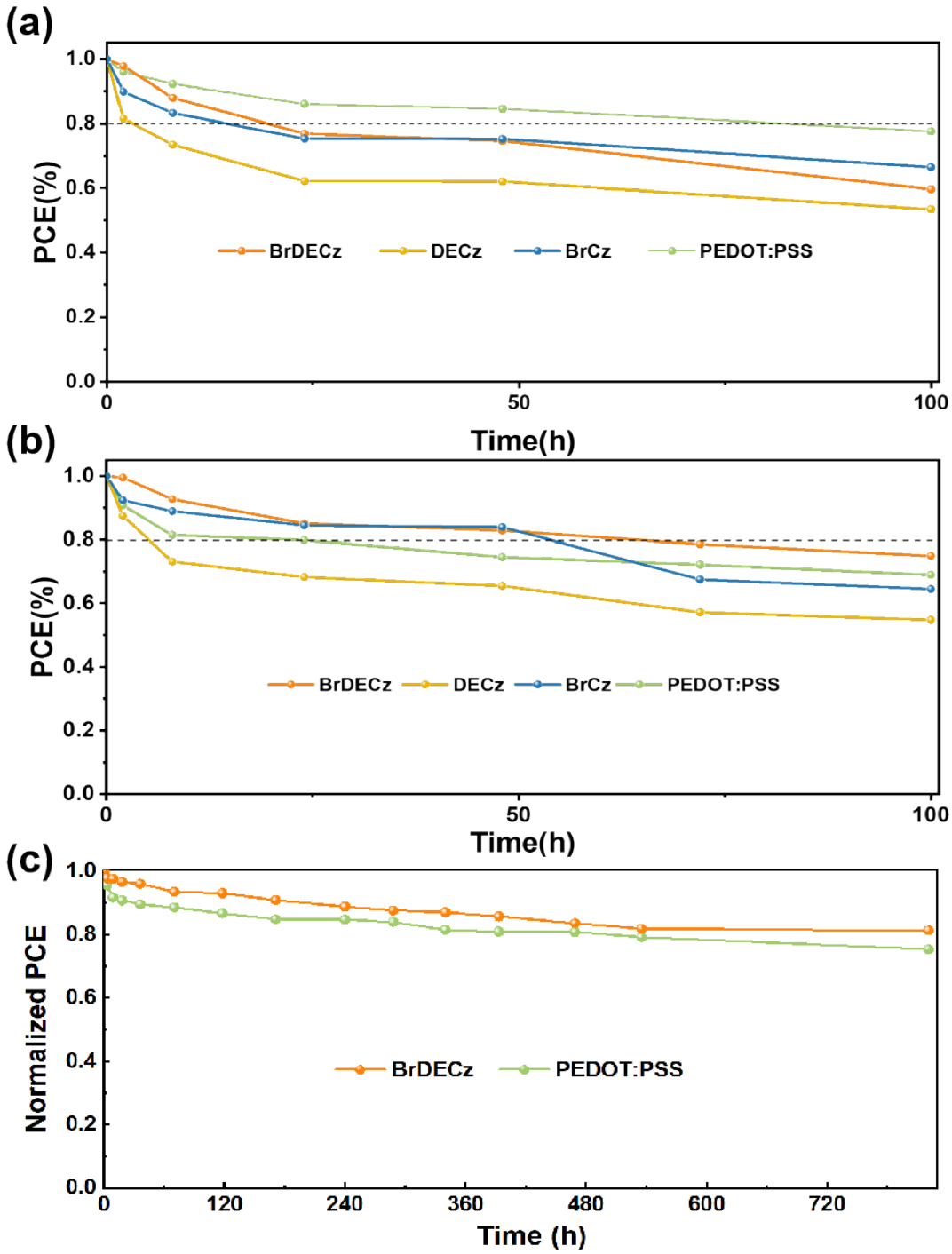

Figure S10. (a) The device stability under UV light. (b) The device stability under simulated sunlight. (c) Normalized PCE decay of the unencapsulated devices based on PEDOT: PSS and BrDECz heated at 85℃ in the glovebox.

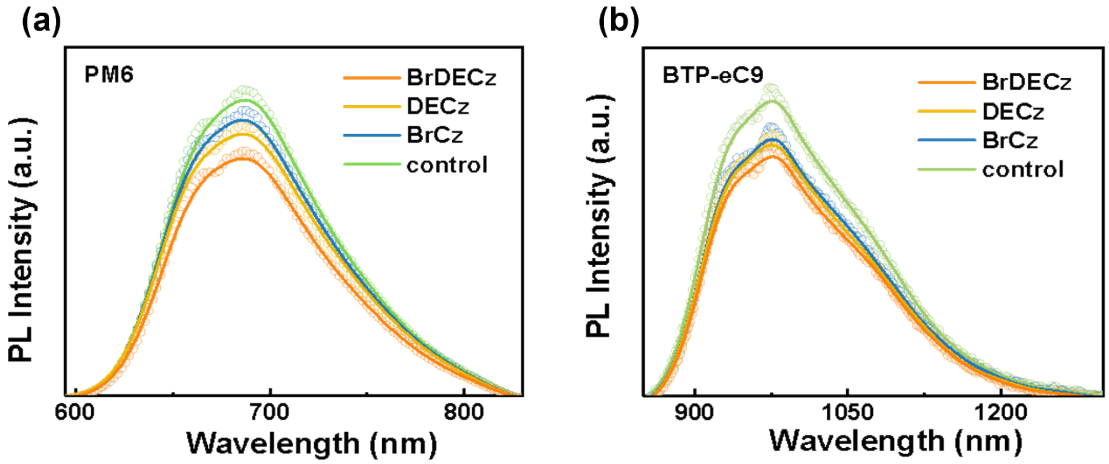

Figure S11. PL emission of PM6 and BTP-eC9 neat film with BrCz, DECz and BrDECz SAMs under 450 nm excitation.

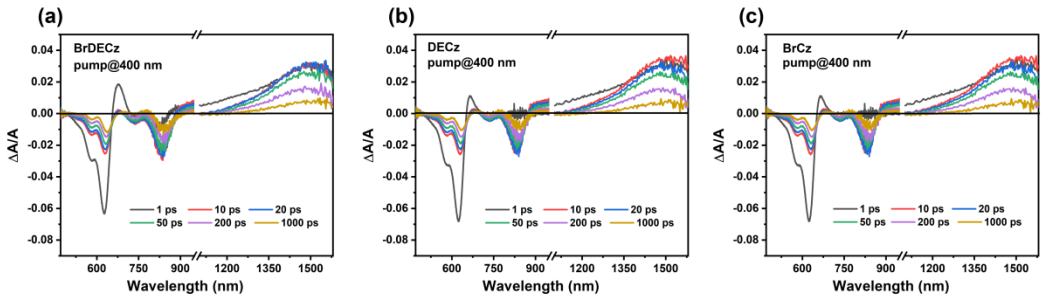

Figure S12. Line-cuts of fs-TAS at indicated delay times.

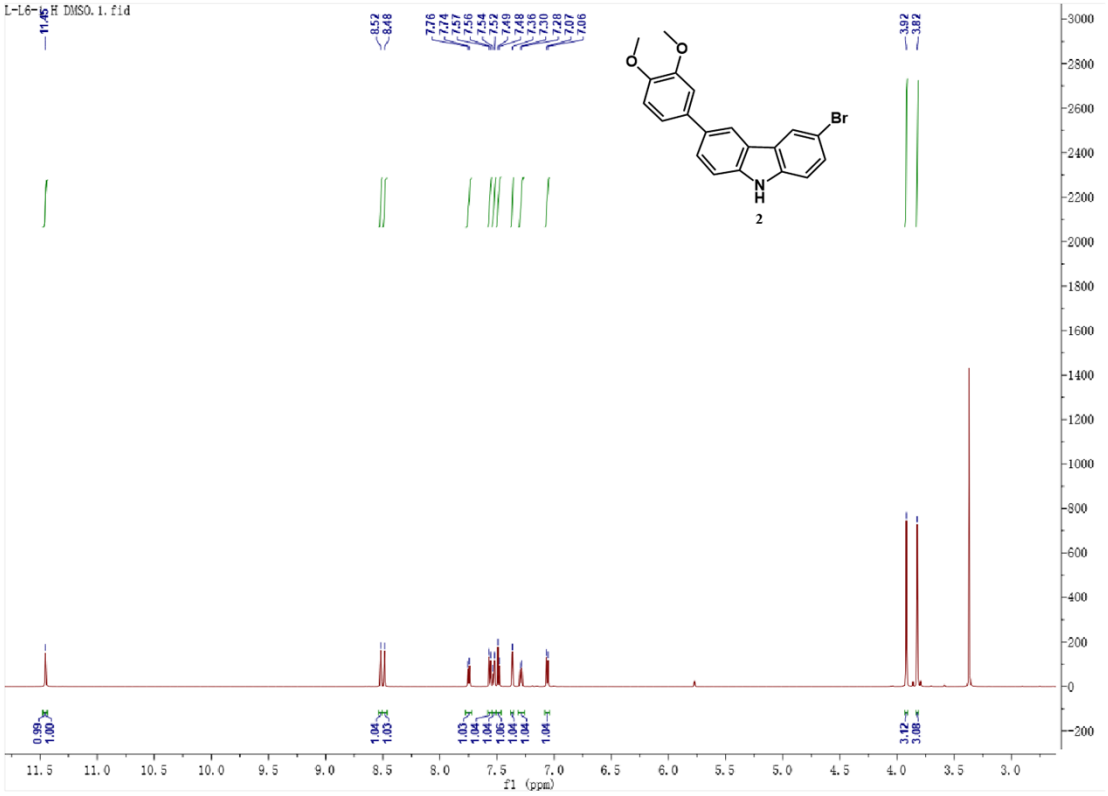

Figure S13. ^{1}H NMR spectra of 2.

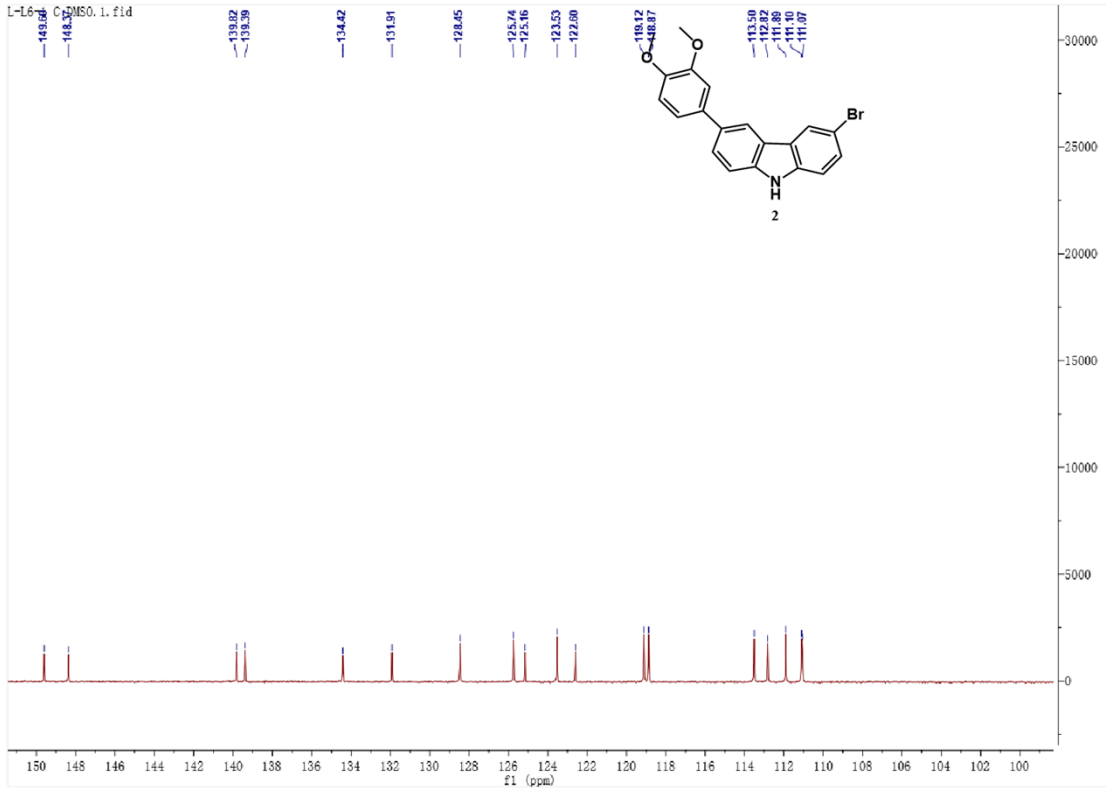

Figure S14. ^{13}C NMR spectra of 2.

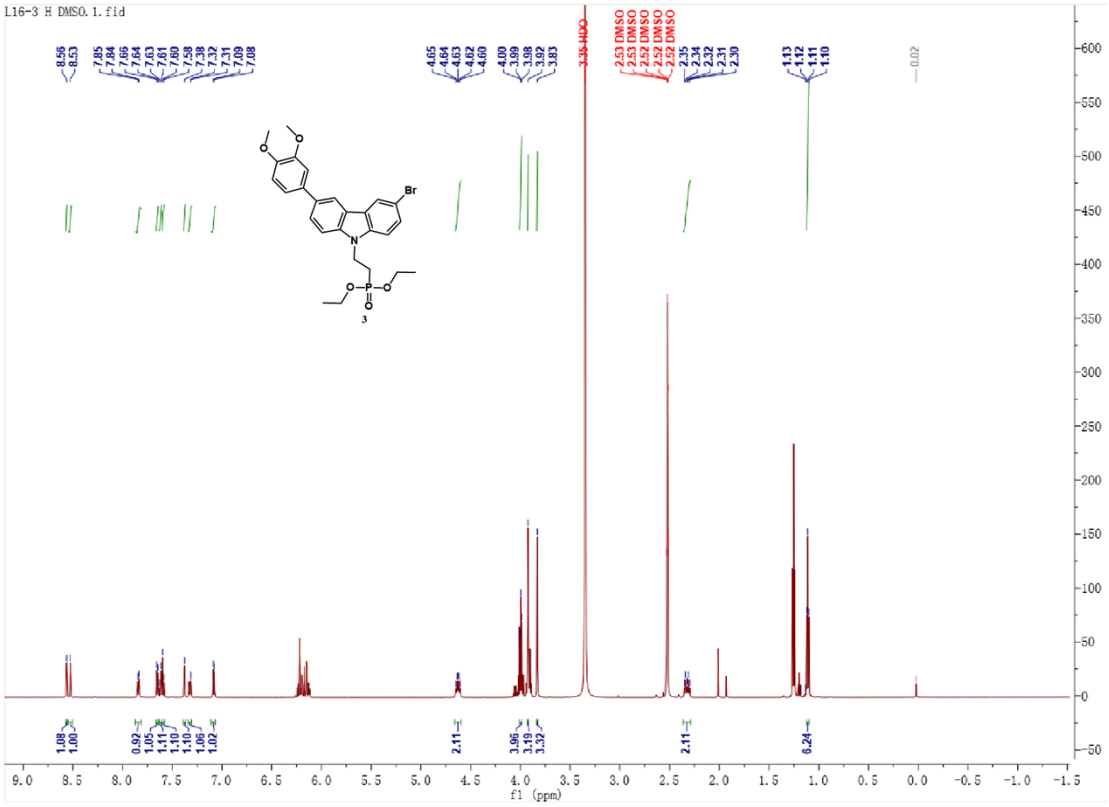

Figure S15. ^{1}H NMR spectra of 3.

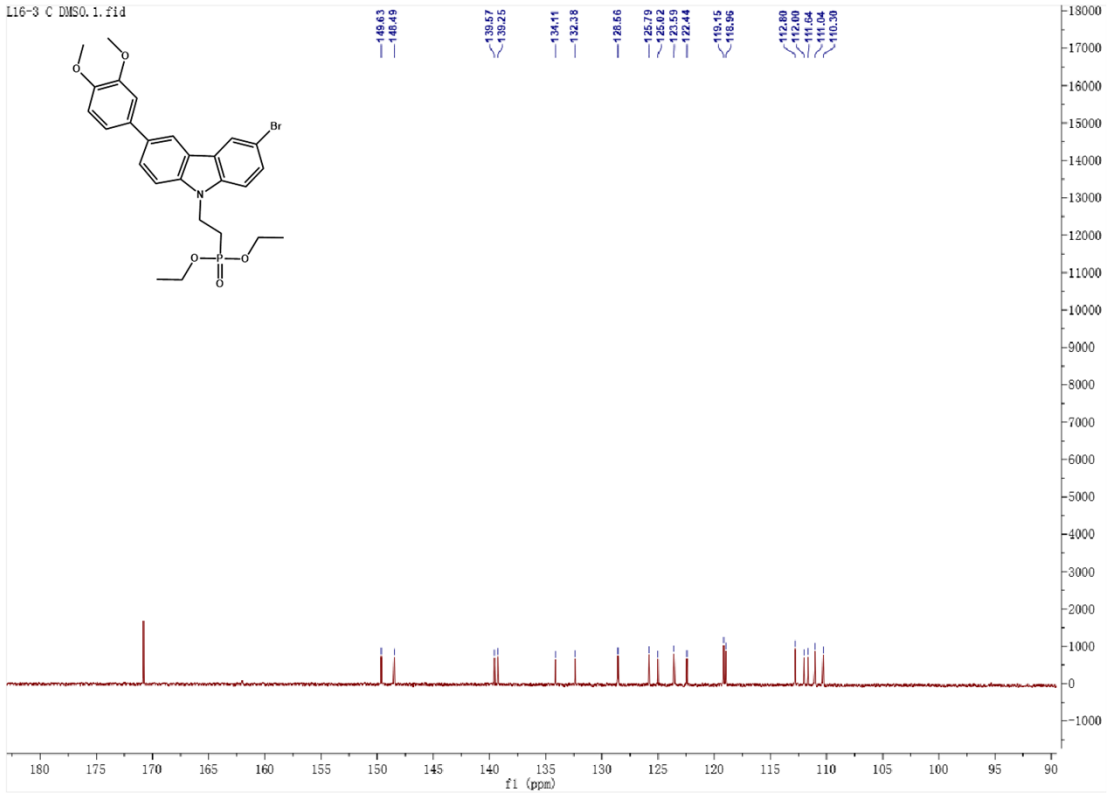

Figure S16. ^{13}C NMR spectra of 3.

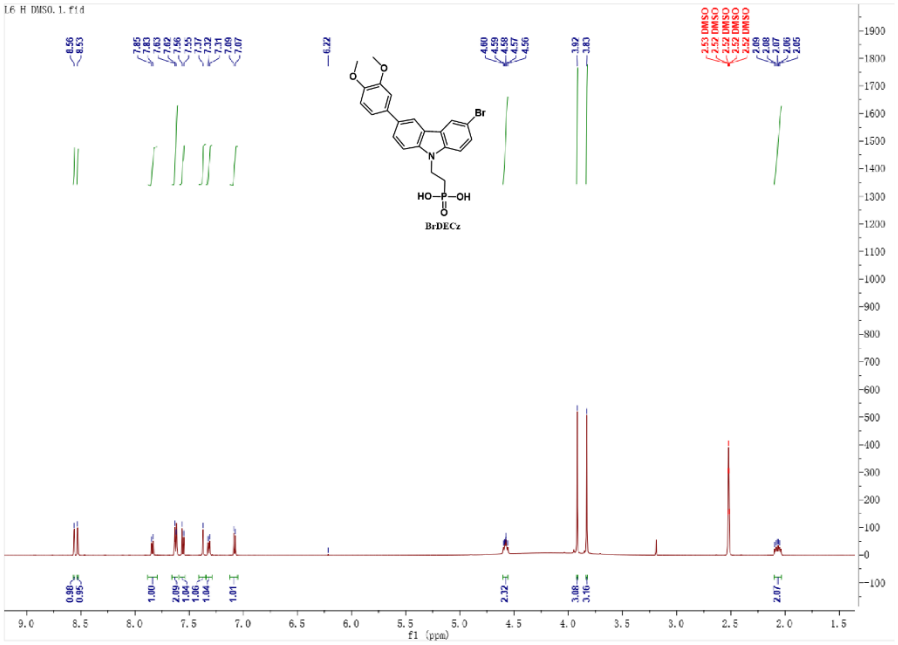

Figure S17. ^{1}H NMR spectra of BrDECz.

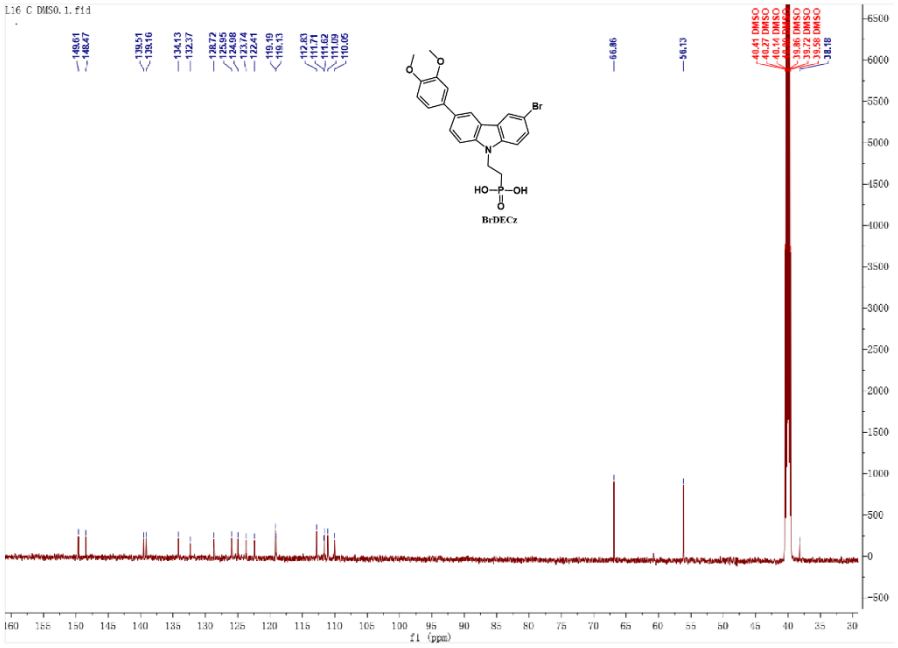

Figure S18. ^{13}C NMR spectra of BrDECz.

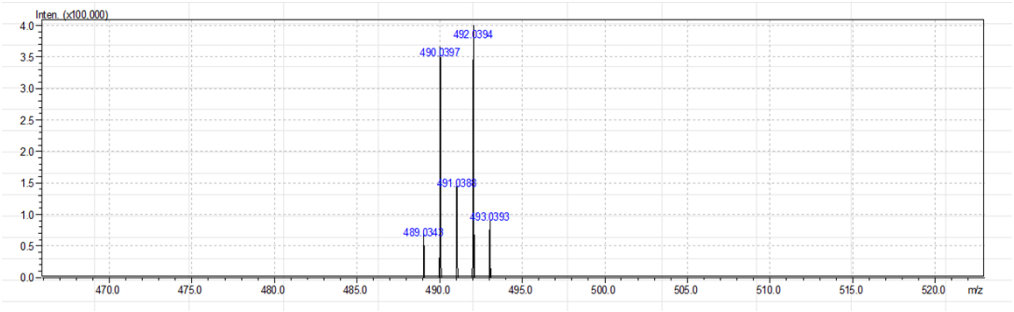

Figure S19. HRMS spectra of BrDECz.

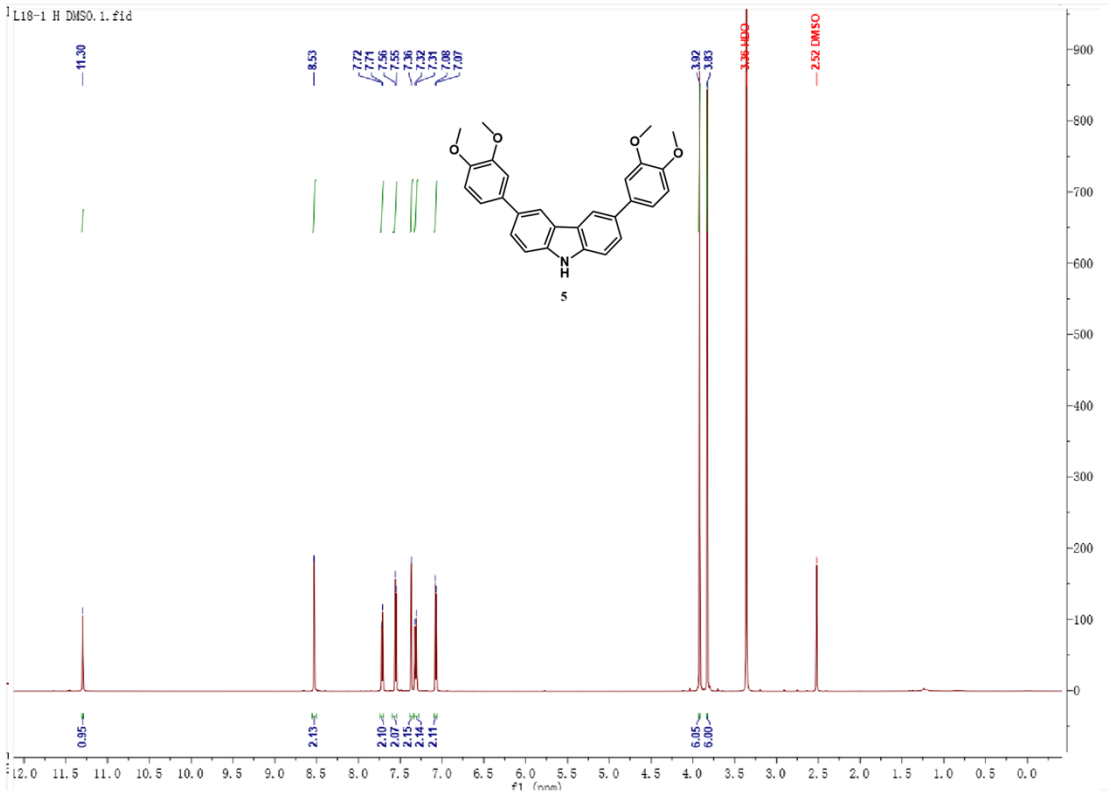

Figure S20. ^{1}H NMR spectra of 5.

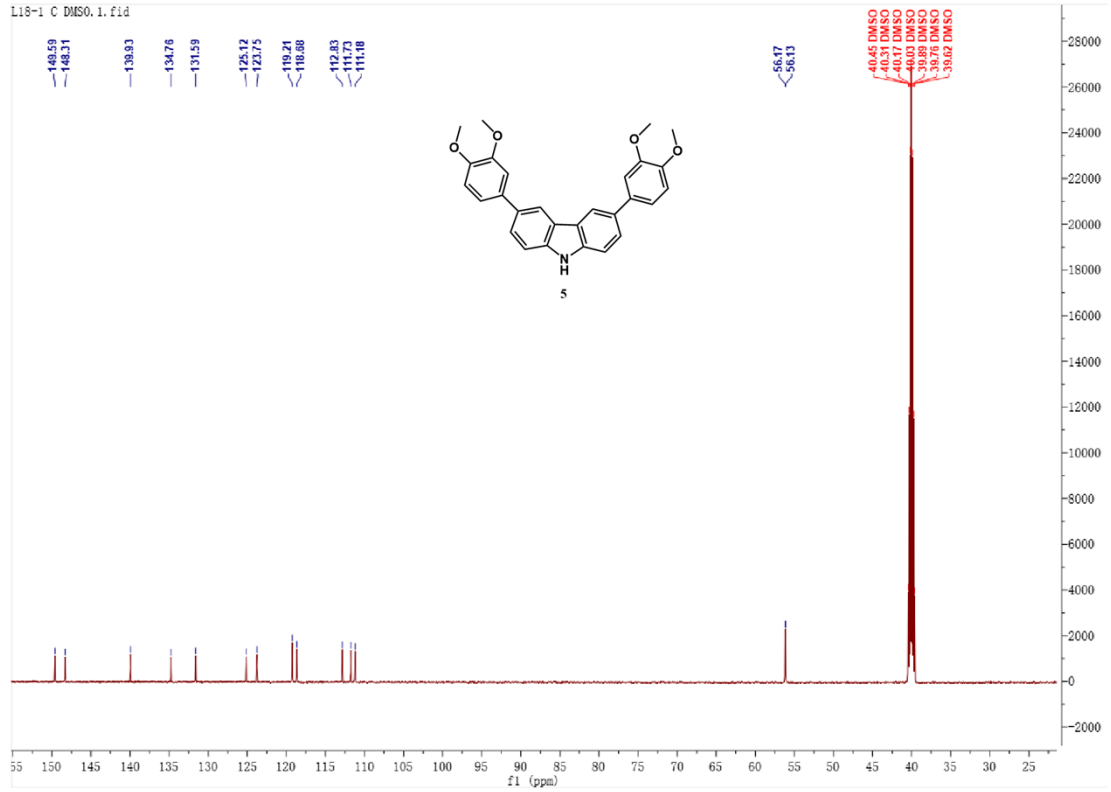

Figure S21. ^{13}C NMR spectra of 5.

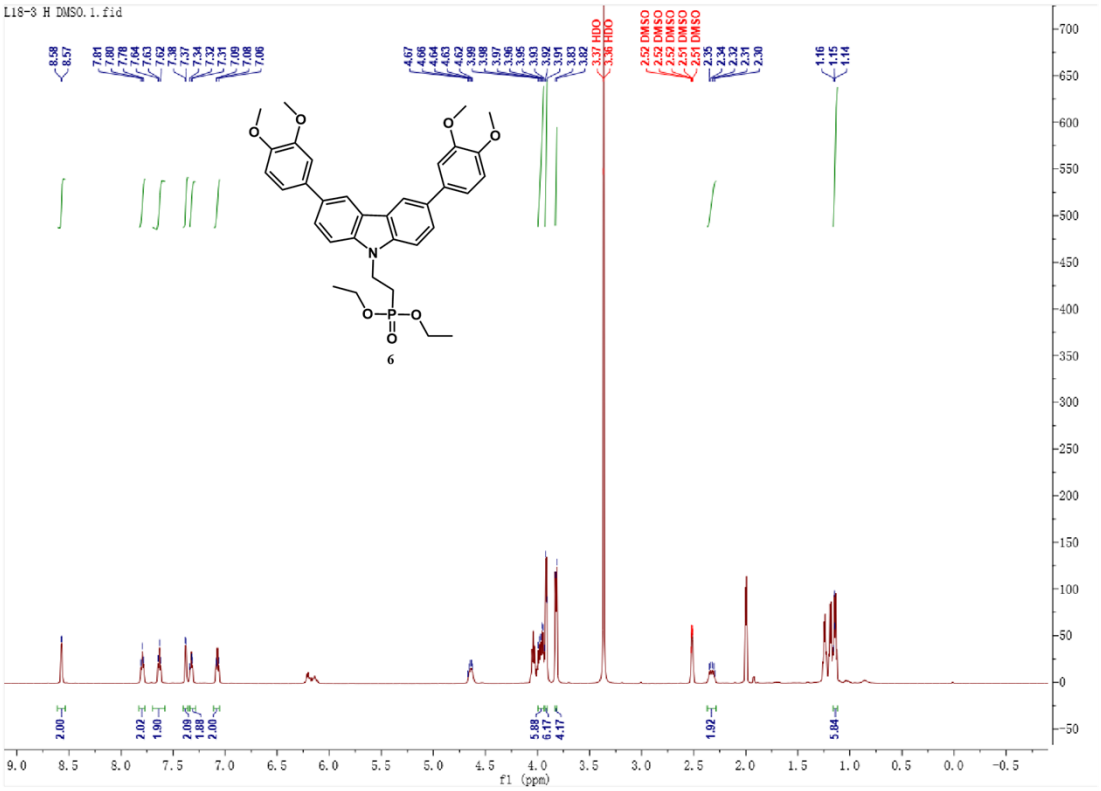

Figure S22. ^{1}H NMR spectra of 6.

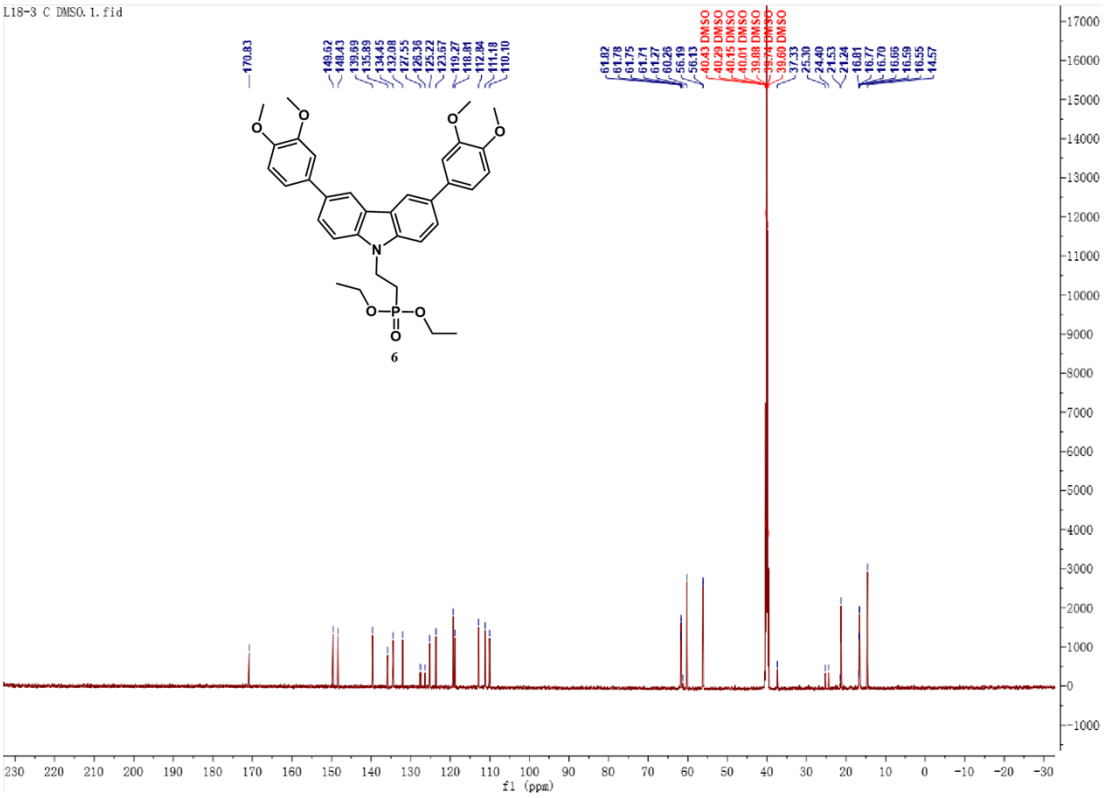

Figure S23. ^{13}C NMR spectra of 6.

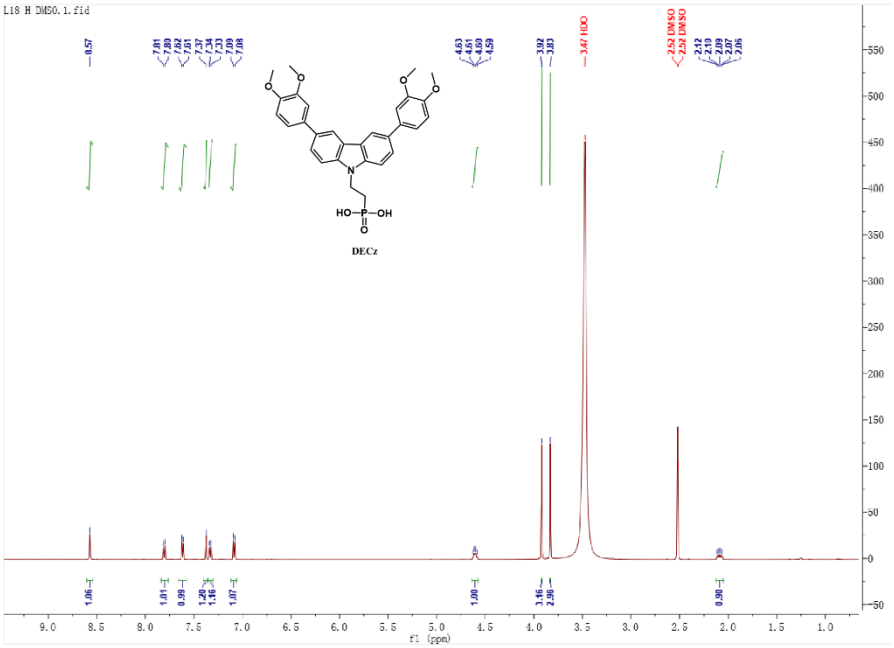

Figure S24. ^{1}H NMR spectra of DECz.

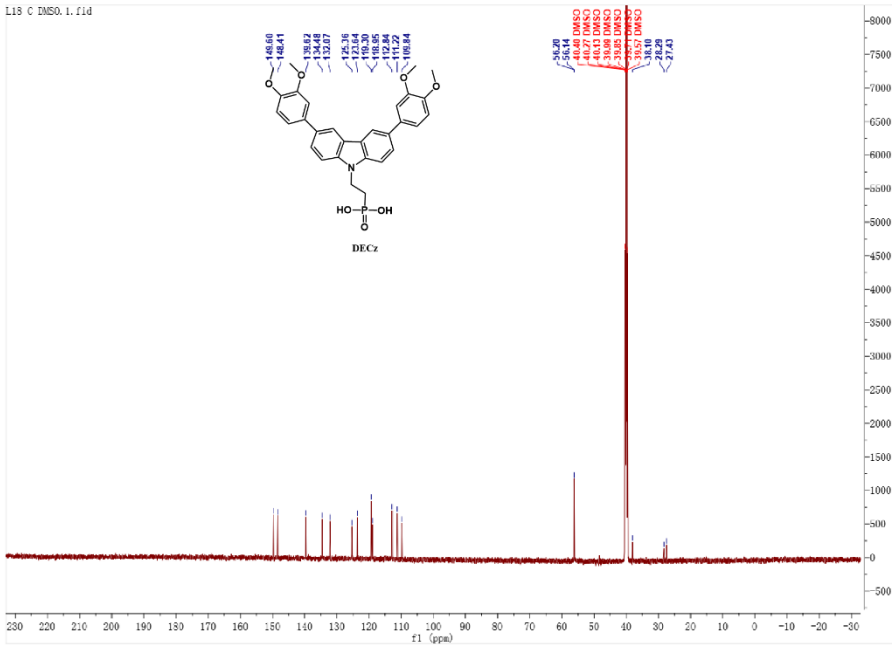

Figure S25. ^{13}C NMR spectra of DECz.

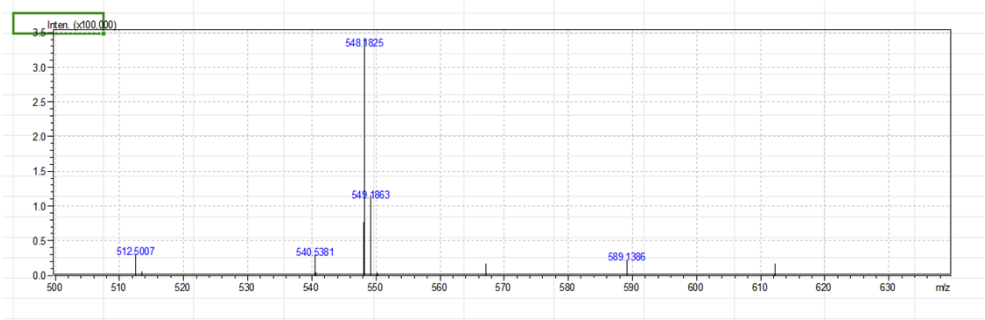

Figure S26. HRMS spectra of DECz.

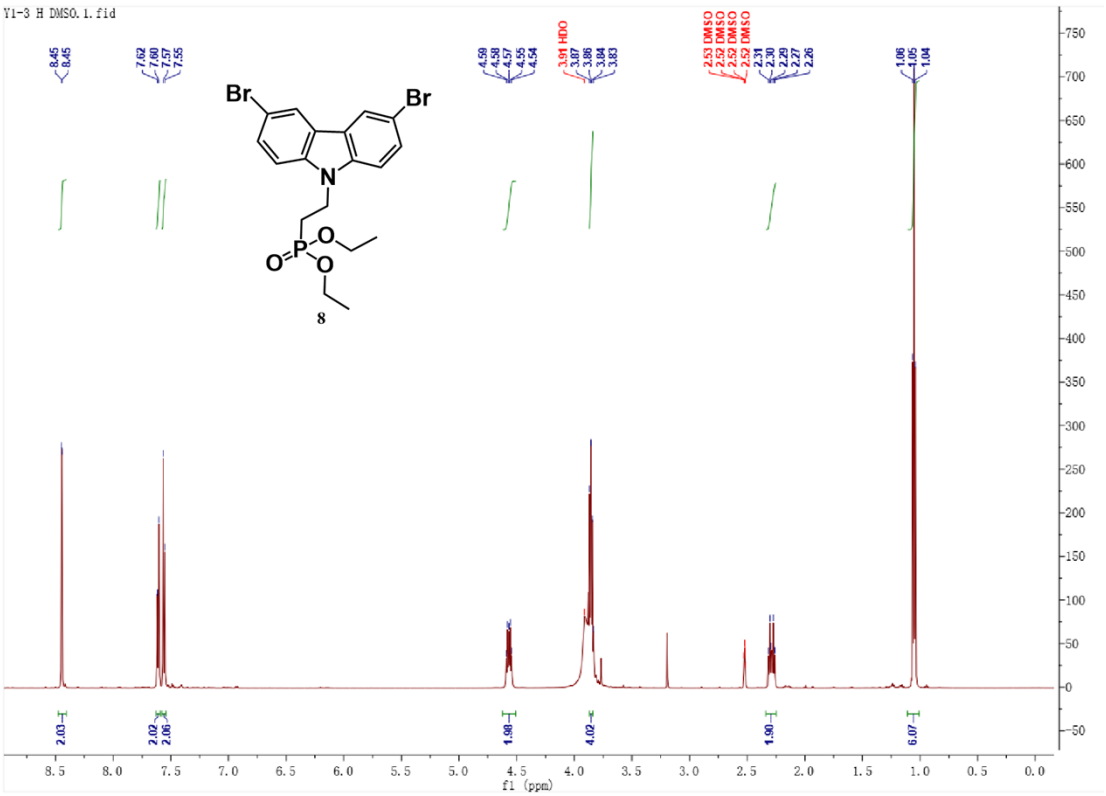

Figure S27. ^{1}H NMR spectra of 8.

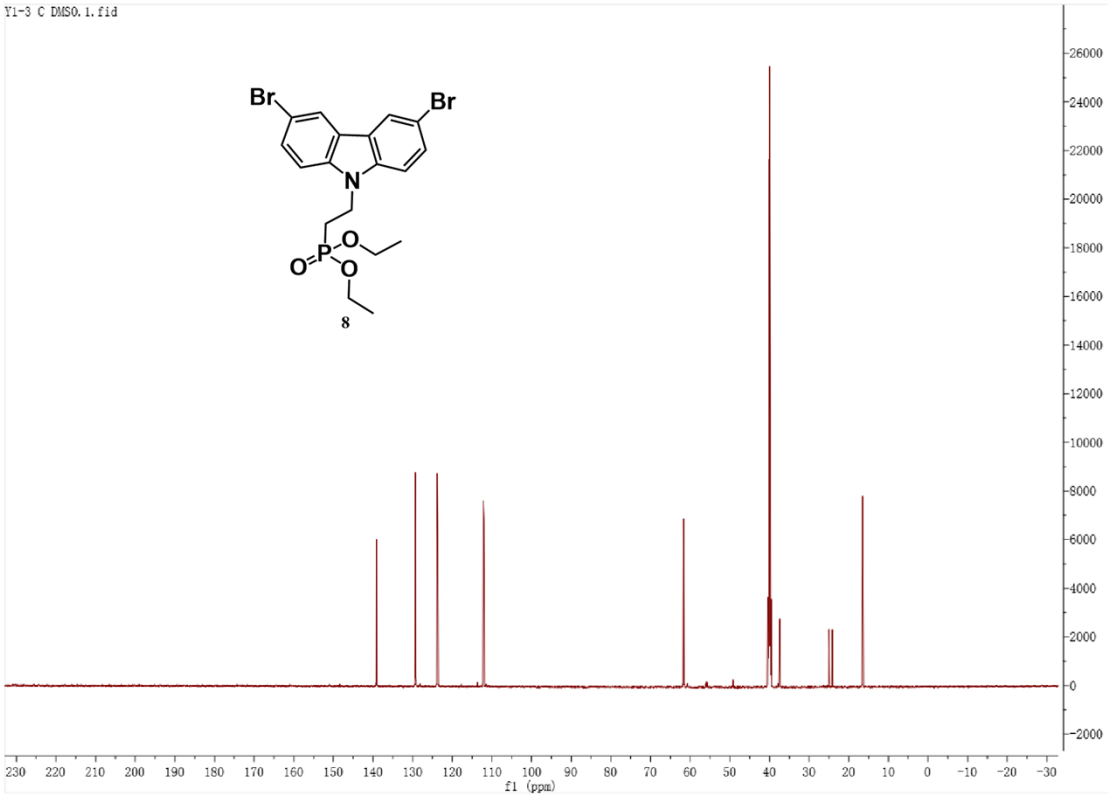

Figure S28. ^{13}C NMR spectra of 8.

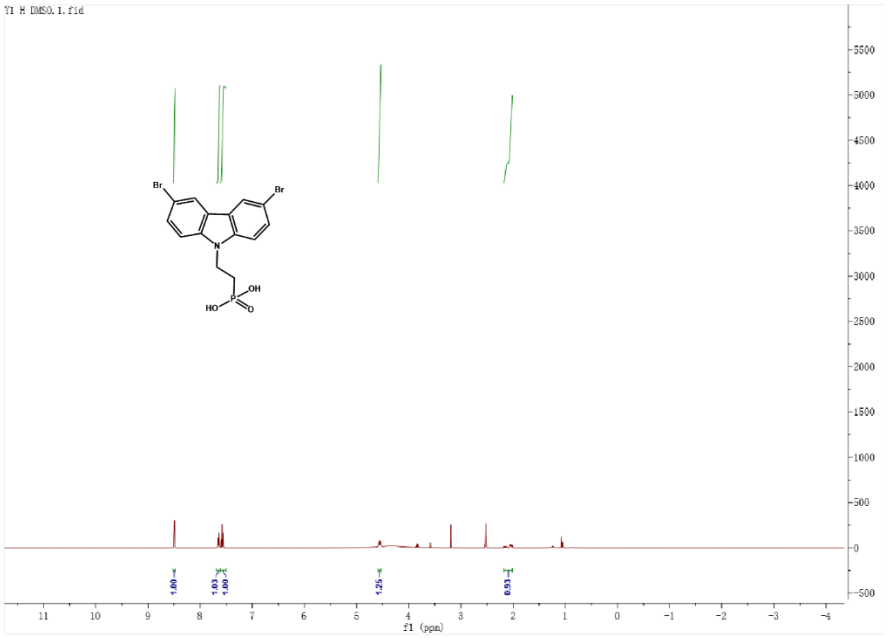

Figure S29. ^{1}H NMR spectra of BrCz.

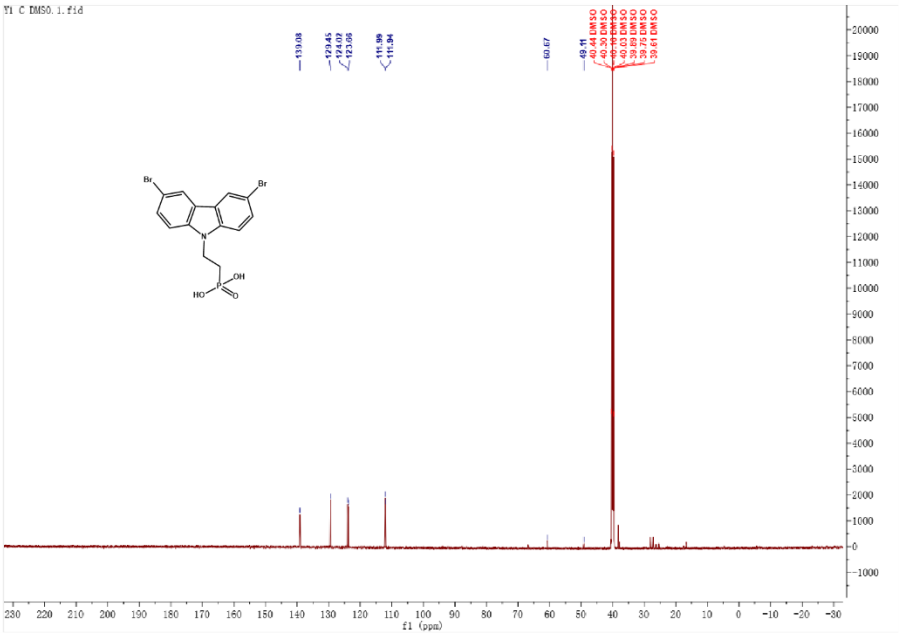

Figure S30. ^{13}C NMR spectra of BrCz.

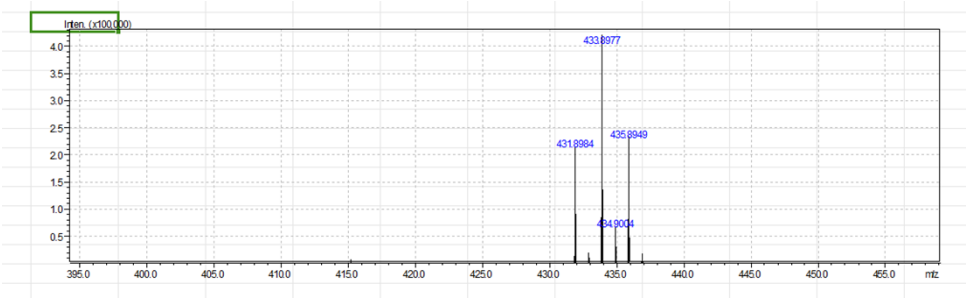

Figure S31. HRMS spectra of BrCz.

13. Supporting Tables

Table S1. Optimized concentration of BrDECz.

SAM	Concentration	*V*oc (V)	J_{SC}(mA cm^{-2})	FF	PCE (%)
BrDECz	0.3	0.85	28.03	75.58	18.02
	0.3	0.86	28.88	76.09	18.85
BrDECz	0.4	0.86	29.22	77.84	19.56
	0.4	0.87	28.85	78.37	19.67
BrDECz	0.5	0.87	28.47	77.68	19.15
	0.5	0.86	28.84	77.50	19.32

Table S2. Optimized concentration of DECz.

SAM	Concentration	*V*oc (V)	J_{SC}(mA cm^{-2})	FF	PCE (%)
DECz	0.3	0.85	28.75	72.83	17.82
	0.3	0.84	29.05	72.37	17.81
DECz	0.4	0.85	29.28	76.21	18.99
	0.4	0.85	29.17	76.43	18.86
DECz	0.5	0.85	28.80	75.94	18.58
	0.5	0.84	28.55	75.86	18.30

Table S3. Optimized concentration ofBrCz.

SAM	Concentration	*V*oc (V)	J_{SC}(mA cm^{-2})	FF	PCE (%)
BrCz	0.3	0.85	28.40	76.49	18.61
	0.3	0.85	28.39	76.79	18.57
BrCz	0.4	0.85	27.77	72.94	17.34
	0.4	0.85	27.71	73.53	17.38
BrCz	0.5	0.85	27.59	73.39	17.30
	0.5	0.85	28.17	72.20	17.41

Table S4. Summary of the fitting parameter used to describe the Nyquist plots.

Electrodes	Rs	R_{bulk}
ITO/BrDECz	27.7	2.8K
ITO/BrCz	23.9	1.9K
ITO/DECz	17.2	3.8K

Table S5. A summary of reported PCE values for conventional OSCs with SAM interfaces.

SAMs	BHJ	*Voc* (V)	PCE (%)	Ref.
Cl-2PACz	PM6:PM7-Si: BTP-eC9:BV	0.866	18.9	[4]
BPC-M	PBDB-TF: BTP-eC9	0.856	19.3	[5]
BrBACz	PM6: BTP-eC9	0.856	19.7	[6]
4,5-Cl-2PACz	PM6: BTP-eC9:L8-BO-F	0.856	19.05	[7]
Br-2PACz	PM6: BTP-eC9: $PC_{71}BM$	0.864	18.4	[8]
3-BPIC-F	PM6:L8-BO: BTP-ec9	0.872	19.71	[9]
Poly-2PACz	PM6: PTQ10: L8-BO	0.87	19.1	[10]
2PACz	PM6: BTP-ec9: $PC_{71}BM$	0.845	18.03	[11]
BrDECz	PM6: BTP-eC9	0.87	19.67	This work

Table S6. The effect of interfacial materials on various active layer systems.

SAMs	BHJ	*Voc* (V)	*Jsc* (mA cm^{-2})	FF (%)	PCE (%)
PM6:Y6	BrDECz	0.85	28.01	76.46	18.29
	DECz	0.83	28.01	75.94	17.65
	BrCz	0.84	28.04	75.65	17.81
	PEDOT:PSS	0.85	27.56	74.16	17.38
PM6:L8BO	BrDECz	0.89	26.75	76.77	18.23
	DECz	0.88	26.20	77.09	17.83
	BrCz	0.88	26.13	76.68	17.52
	PEDOT:PSS	0.89	24.98	76.89	17.03
PM6:BTP-eC9	BrDECz	0.87	28.85	78.32	19.67
	DECz	0.85	28.64	77.00	18.74
	BrCz	0.85	28.40	76.49	18.46
	PEDOT:PSS	0.85	28.10	76.34	18.29
B1:BTP-eC9	BrDECz	0.81	26.63	74.36	16.05
	DECz	0.81	26.15	73.43	15.59
	BrCz	0.81	26.13	71.01	15.19
	PEDOT:PSS	0.81	26.10	71.18	15.09

Table S7. The costs associated with the synthesis of the unsymmetrical interfacial materials.

Organic Reagents	**Unit price (¥/g)**	**Quantity used (g)**	**Cost (¥)**
3,6-dibromocarbazole	1.02	1	1.02
3,4-dimethoxyphenylboronic acid	5.6	0.8	4.48
Diethyl 2-bromoethylphosphonate	7	0.4	2.8
Bromotrimethylsilane	6.6	0.4	2.64
$Pd(PPh_3)_4$	3.2	0.05	0.16
Inorganic Reagents	**Unit price (¥/g)**	**Quantity used (g)**	**Cost (¥)**
K_2CO_3	0.096	0.5	0.048
Silica gel	0.02	150	3
Solvent	**Unit price (¥/ml)**	**Quantity used (g)**	**Cost (¥)**
Dioxane	0.058	25	1.45
Dichloromethane	0.018	230	4.14
Petroleum ether	0.011	200	2.2
Ethyl acetate	0.014	500	7
Dimethyl sulfoxide	0.072	25	1.8
Product	**Unit price (¥/g)**	**Quantity yield (g)**	**Cost (¥)**
BrDECz	153.65	0.2	30.738

14. References

1. D. R. Meena, S. R. Gadre and P. Balanarayan, *Comput. Phys. Commun.*, 2018, **224**, 299-310.
2. S. Kadkhodaei and A. van de Walle, *Comput. Phys. Commun.*, 2020, **246**, 106712.
3. Z.-L. Liu, C. E. Ekuma, W.-Q. Li, J.-Q. Yang and X.-J. Li, *Computer Physics Communications*, 2022, **270**, 108180.
4. Y. Lin, Y. Zhang, J. Zhang, M. Marcinskas, T. Malinauskas, A. Magomedov, M. I. Nugraha, D. Kaltsas, D. R. Naphade, G. T. Harrison, A. El-Labban, S. Barlow, S. De Wolf, E. Wang, I. McCulloch, L. Tsetseris, V. Getautis, S. R. Marder and T. D. Anthopoulos, *Adv. Energy Mater.*, 2022, **12**, 2202503.
5. Z. Chen, S. Zhang, T. Zhang, J. Dai, Y. Yu, H. Li, X. Hao and J. Hou, *Joule*, 2024, **8**, 1723-1734.
6. X. Yu, P. Ding, D. Yang, P. Yan, H. Wang, S. Yang, J. Wu, Z. Wang, H. Sun, Z. Chen, L. Xie and Z. Ge, *Angew. Chem.-Int. Edit.*, 2024, **63**, e202401518.
7. Y. Wang, W. Jiang, S.-C. Liu, C.-T. Lin, B. Fan, Y. Li, H. Gao, M. Liu, F. R. Lin and A. K.-Y. Jen, *Adv. Energy Mater.*, 2024, **14**, 2303354.
8. Y. Lin, A. Magomedov, Y. Firdaus, D. Kaltsas, A. El-Labban, H. Faber, D. R. Naphade, E. Yengel, X. Zheng, E. Yarali, N. Chaturvedi, K. Loganathan, D. Gkeka, S. H. AlShammari, O. M. Bakr, F. Laquai, L. Tsetseris, V. Getautis and T. D. Anthopoulos, *ChemSusChem*, 2021, **14**, 3569-3578.
9. H. Liu, Y. Xin, Z. Suo, L. Yang, Y. Zou, X. Cao, Z. Hu, B. Kan, X. Wan, Y. Liu and Y. Chen, *J. Am. Chem. Soc.*, 2024, **146**, 14287-14296.
10. Z. Ren, S. Luo, X. Shi, Y. Dou, T. Liu, L. Wang, K. K. Tsang, F. Wang, Y. Zhao, Y. Liu, X. Hu, X. Peng, W. Liu, H. Yan and S. Chen, *Sci. China: Chem.*, 2024, **67**, 1941-1945.
11. Y. Lin, Y. Firdaus, F. H. Isikgor, M. I. Nugraha, E. Yengel, G. T. Harrison, R. Hallani, A. El-Labban, H. Faber, C. Ma, X. Zheng, A. Subbiah, C. T. Howells, O. M. Bakr, I. McCulloch, S. D. Wolf, L. Tsetseris and T. D. Anthopoulos, *ACS Energy Lett.*, 2020, **5**, 2935-2944.